CORTEX 129 (2020) 423–435

Available online at www.sciencedirect.com

ScienceDirect

Journal homepage: www.elsevier.com/locate/cortex

Single Case Report

Altered large-scale organization of shape processing in visual agnosia

Erez Freud [a,*,1] and Marlene Behrmann [b]

[a] Department of Psychology and Centre for Vision Research, York University, Toronto, ON, Canada
[b] Department of Psychology and the Carnegie Mellon Neuroscience Institute, Carnegie Mellon University, Pittsburgh, PA, USA

ARTICLE INFO

Article history:
Received 11 November 2019
Reviewed 7 February 2020
Revised 29 February 2020
Accepted 4 May 2020
Action editor Thomas Schenk
Published online 25 May 2020

Keywords:
Visual agnosia
Object recognition
Two visual pathways
fMRI

ABSTRACT

Recent findings suggest that both dorsal and ventral visual pathways process shape information. Nevertheless, a lesion to the ventral pathway alone can result in visual agnosia, an impairment in shape perception. Here, we explored the neural basis of shape processing in a patient with visual agnosia following a circumscribed right hemisphere ventral lesion and evaluated longitudinal changes in the neural profile of shape representations. The results revealed a reduction of shape sensitivity slopes along the patient's right ventral pathway and a similar reduction in the contralesional left ventral pathway. Remarkably, posterior parts of the dorsal pathway bilaterally also evinced a reduction in shape sensitivity. These findings were similar over a two-year interval, revealing that a focal cortical lesion can lead to persistent large-scale alterations of the two visual pathways. These alterations are consistent with the view that a distributed network of regions contributes to shape perception.

1. Introduction

Shape processing is a cornerstone of many perceptual behaviors such as object recognition, face perception and orthographic processing. For decades, shape perception has been considered the sole product of computations carried out by the ventral visual pathway. However, recent research has demonstrated that regions along the dorsal visual pathway, which is usually associated with visuomotor control (Gallivan & Culham, 2015), also derive shape representations (Freud, Culham, et al., 2017; Vaziri-Pashkam & Xu, 2018; Konen & Kastner, 2008; Bracci & Op de Beeck, 2016; for a review see, Freud, Plaut, & Behrmann, 2016). These dorsal representations have their own unique temporal dynamics (Collins, Freud, Kainerstorfer, Cao, & Behrmann, 2019), and are correlated with perceptual behaviors (Freud, Culham, et al., 2017; Freud, Robinson, et al., 2018).

* *Corresponding author*. Department of Psychology and the Centre for Vision Research, York University, 4700 Keele Street, Toronto, Ontario, M3J 1P3 Canada.
E-mail address: efreud@yorku.ca (E. Freud).
[1] Office: Sherman Health Science Research Centre, room 1008.
https://doi.org/10.1016/j.cortex.2020.05.009
0010-9452/

An outstanding question, then, concerns the relationship between the object representations derived by the two pathways. One view is that the two pathways derive independent representations, an account that can easily explain the reported functional dissociation (i.e., perception *vs* action) between the ventral and dorsal pathways (Goodale, Milner, Jakobson, & Carey, 1991). Given the independence of processing, a lesion to one pathway should have no impact on the representations derived by the other pathway. This architecture of independence, however, is neither supported by functional (Freud, Rosenthal, Ganel, & Avidan, 2015; Garcea, Chen, Vargas, Narayan, & Mahon, 2018; Mahon, Kumar, & Almeida, 2013) nor anatomical (Yeatman et al., 2014) studies which reveal strong structural and functional connections between the two pathways.

An alternative account is one in which the dorsal pathway representations (particularly for tasks with no visuomotor component) are merely the result of computations carried out by the ventral pathway. This view predicts that a lesion to the ventral pathway would adversely affect the representation derived by the dorsal pathway, but not vice versa. Recent findings challenge this view, as shape sensitivity along the dorsal pathway can temporally precede the emergence of shape sensitivity along the ventral pathway (Collins et al., 2019). Moreover, a transient inactivation of the dorsal pathway (i.e., caudal intraparietal sulcus (CIP)) in monkeys can lead to reduction in fMRI activation of the ventral pathway and to perceptual deficits in 3D perception (Van Dromme, Premereur, Verhoef, Vanduffel, & Janssen, 2016).

Finally, a third plausible perspective suggests that both pathways derive object representations. These representations may or may not be identical and, if the latter, might encode distinctive information about objects which may serve different functional goals (Freud, Behrmann, & Snow, 2020). In either case, however, the two pathways are interactive and, therefore, a lesion to either pathway should affect the representations derived by the other pathway.

In a previous paper, we also investigated the status of the dorsal and ventral pathways with respect to each other, and demonstrated that, in patients with visual agnosia following a lesion to the ventral pathway, the dorsal pathway continues to evince sensitivity to object 3D structure and this is true even in a case with a very extensive bilateral ventral lesion (Freud, Ganel, et al., 2017). This finding might be taken as support for the first account, namely, that of independent object representations. However, it is important to note, that this study focused only on one, high-level visual property, and that was shape (i.e., 3D structure). Additionally, the fMRI analysis was focused on only two ROIs along the dorsal pathway, and therefore, it is unclear if and to what extent other regions along the dorsal pathway may be affected by a lesion to the ventral pathway.

In the current study, we sought to provide a comprehensive examination of both visual pathways in a patient with visual agnosia, SM, following a lesion to the right ventral pathway. By employing a parametric scrambling manipulation (Collins et al., 2019; Freud, Culham, et al., 2017; Freud, Plaut, & Behrmann, 2019; Grill-Spector et al., 1998; Lerner, Hendler, Ben-Bashat, Harel, & Malach, 2001; Malach et al., 1995), we altered the availability of shape information shown to participants and collected BOLD data at the same time. We then generated a detailed description of shape processing in all visually selective voxels along the entirety of both visual pathways and compared the profile of the patient to that of a group of healthy controls. Last, we collected behavioral data and correlated this with the functional BOLD profile.

1.1. *The durability of stored visual representations*

In addition to characterizing the representations derived by each of the two pathways, we had the opportunity to evaluate any changes in the neural sensitivity to shape information over the course of a two-year interval and the reliability of the findings over time.

To date, there have been few studies of visual agnosia for whom longitudinal data are available and all of these cases appear to have little, if any, improvement. One case with visual agnosia as a result of a traumatic brain injury showed little change over a 10 year period with perhaps minimally better reading and drawing than writing and copying (Kertesz, 1979). A second case, HJA (Humphreys & Riddoch, 1984, 1987; Riddoch & Humphreys, 1987), showed minor improvement in his perceptual abilities over a 16 year period although he did improve in naming real objects but this appeared to result from compensatory use of 3D, color and texture information (Riddoch, Humphreys, Gannon, Blott, & Jones, 1999, 2003). Most relevant is that, over time, HJA showed *deterioration* of his long-term knowledge of the visual properties of objects, a finding taken to indicate that perceptual encoding may be necessary to ensure the maintenance of stored visual representations. The remaining two cases are reported to show some recovery over time, for example, in recognizing line drawings in patient JR, when assessed 10 years after the initial insult (Davidoff & Wilson, 1985; Wilson & Davidoff, 1993), or in identifying overlapping figures in patient HC, evaluated several times including at 40 years post injury (Adler, 1944, 1950; Sparr, Jay, Drislane, & Venna, 1991). Close scrutiny of these cases suggests that long term visual representations might have degraded over time; for example, both JR's and HC's drawings were remarkably coarse and simplistic and, furthermore, JR appeared to know rather little about the physical appearance of objects, potentially indicating the deterioration of stored visual representations. Together, these cases seem to argue for the necessity of bottom-up activation to ensure the robustness of long-term visual representations. We note, however, that none of these studies explored changes in functional imaging data over time and so information about the neural profile over time is not available. To shed further light on the possible interdependence of perceptual and mnemonic representations, here, we examine any possible longitudinal changes in the neural correlates of shape perception in SM. We do acknowledge that insights gained over time in SM might not be especially fruitful given that this study was initiated after he had been agnosic for roughly two decades and his agnosia might be unlikely to change once such stability had been achieved.

2. Materials and methods

We report how we determined our sample size, all data exclusions (if any), all inclusion/exclusion criteria, whether inclusion/exclusion criteria were established prior to data analysis, all manipulations, and all measures in the study. All data that are necessary and sufficient to replicate all analyses and data presentations in the current article are publicly archived at 10.1184/R1/c.4967927.

2.1. Participants

All participants had normal or corrected-to-normal vision and none had remarkable psychiatric or neurological histories. Participants provided informed consent to participate in the protocol, which was approved by the Institutional Review Board of Carnegie Mellon University. We compensated all participants for their participation.

2.2. Patient SM

SM was 40 and 42 years old when he completed the two scans described here. He sustained a closed head injury in a motor vehicle accident at the age of 18. Clinical CT scans acquired close to the time of the injury indicated a contusion in the right anterior and posterior temporal cortex accompanied by a shearing injury in the corpus callosum and left basal ganglia. A 3T MRI scan from 2009 revealed a circumscribed lesion in right occipito-temporal cortex in the vicinity of area LOC (for detailed lesion demarcation, see (Konen, Behrmann, Nishimura, & Kastner, 2011)) and this is confirmed in the current paper (see Fig. 1).

SM recovered well from the traumatic brain injury after lengthy rehabilitation, aside from a persisting object agnosia and dense prosopagnosia (Behrmann & Plaut, 2014). SM's visual abilities have been described in detail in previous publications, and the reader is referred to those papers for a more comprehensive account (Freud, Ganel, et al., 2017; Gilaie-Dotan, Saygin, Lorenzi, Rees, & Behrmann, 2015, 2013; Marotta, Genovese, & Behrmann, 2001; Nishimura, Doyle, Humphreys, & Behrmann, 2010). Suffice it to say that SM has normal sensory vision and intact low-level perception (for example, edge orientation and color perception). SM can also perform simple Gestalt grouping operations but is then unable to apprehend a multi-element stimulus as a whole with a specific shape unless there is strong perceptual support for grouping or sufficient time for him to 'solve the puzzle' (his words) (Behrmann & Kimchi, 2003). His object recognition errors reflect the lack of integration of visual parts, for example, labelling a black and white figure of a harmonica a 'computer keyboard' and a tennis racquet 'a fencer's mask'. SM's face recognition impairment appears to be more severe than his object recognition ability, as reflected by his particularly impaired performance on the Benton Facial Recognition Test (32/54; normal 41–54). He is also unable to recognize photographs of any famous people or even of family members, despite being able to provide a good verbal description when presented with their names auditorily.

Structural MRI scans of SM (taken at the current time of testing) reveal a lesion confined to the right ventral occipito-temporal cortex (Fig. 1).

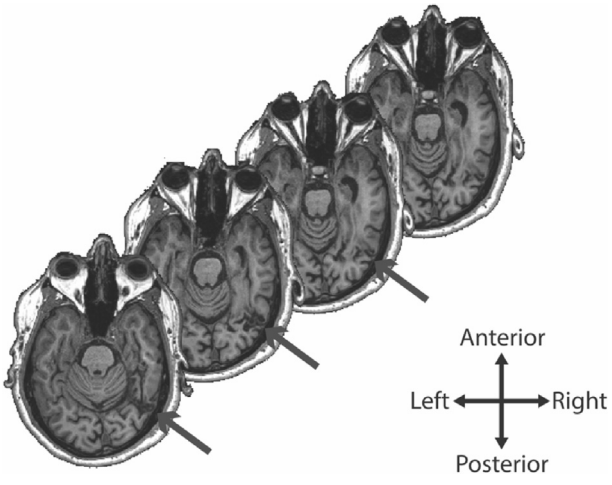

Fig. 1 – Structural scan of patient SM. Representative axial slices from the MRI scan of SM (age 40). The lesion (designated by gray arrows) is observed in the right occipitotemporal lobe.

2.3. Control participants

We utilized the data from Experiment 1 of Freud, Culham, et al. (2017) (11 adult participants) and scanned an additional four participants using the same shape scrambling paradigm to constitute the control group (total N = 15, mean age 29.1, range 19–45, 6 female). Four participants from this group were matched to SM in age (35–45) and sex (male). The data from one additional participant were discarded because of excessive head motion.

2.4. Stimuli

Stimuli were 80 grayscale pictures of forty everyday objects and forty tools identical to those presented in a previous publication (Freud, Culham, et al., 2017). We employed an algorithm that divided and randomly rearranged each intact image into 4, 16, 64 and 256 squares, resulting in five levels of scrambling, labelled S4, S16, S64 and S256 (Fig. 2).

To quantify 'the goodness of shape properties' across the different levels of scrambling we utilized a set of algorithms that measured different shape attributes. We quantified the image entropy (Matlab command: entropy) which provides an estimation of the overall disorder in the image with greater values reflect greater entropy. We found that more scrambled objects were characterized by greater entropy and lower homogeneity (S256 = 2.74; S64 = 2.63; S16 = 2.57; S4 = 2.54; Intact = 2.49).

Additionally, to examine the distortion of high-level shape information (i.e., closed boundaries, continuous counter) we defined the edges of each image by detecting all pixels adjacent to a background (i.e., white) pixel, and then calculated the convex hull, which is the smallest convex set that contains a particular image (Andrew, 1979). Next, for each edge pixel, the distance to the nearest convex hull pixel was computed. The sum of all distances for each image was normalized by dividing

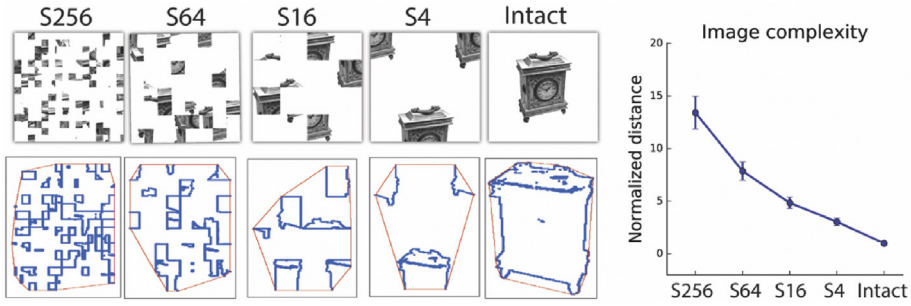

Fig. 2 – Experimental stimuli and a quantitative analysis of 'goodness of shape'. The experimental stimuli consisted of intact objects which were altered by dividing the display using an invisible grid and then randomly rearranging the squares (upper row). Image analysis as a function of scrambling level. For each image, the minimal distance between the shape edges (blue dots) and the image's convex hull (red frame) was computed and normalized relative to the full (intact) image (bottom row). A reduced shape information was observed as a function of the scrambling level (right panel). See Freud, Culham, et al. (2017) and methods for details.

it by the sum of distances for the intact version of that image. Thus, greater values of the normalized distance reflect increased shape complexity relatively to the intact image. Similar to the entropy measure, this procedure confirmed that shape properties were increasingly distorted as a function of the level of scrambling (see Fig. 2 and Freud, Culham, et al., 2017).

3. Experimental design

No part of this study procedures or analyses was pre-registered prior to the research being conducted.

3.1. *MRI setup*

We scanned the participants in a Siemens Verio 3-T magnetic resonance imaging scanner with a 32-channel coil at Carnegie Mellon University. We acquired a structural scan using a T1-weighted protocol that included 176 sagittal slices (1 mm thickness, in-plane resolution = 1 mm, matrix = 256 × 256, repetition time = 2300 msec, echo time = 1.97 msec, inversion time = 900 msec, flip angle = 9°). We employed a gradient-echo, echoplanar imaging sequence (TR = 1.5 sec, TE = 30 msec, flip angle 73°) to acquire the functional images based on the blood oxygenation level-dependent (BOLD) signal. Each run (total of eight) included 227 volumes of 43 axial slices (slice thickness = 3 mm, gap = 0 mm, in-plane resolution = 3 mm).

3.2. *fMRI*

Participants viewed the stimuli (visual angle of 4.5° × 4.5°) in a pseudorandomized order through a mirror setup that reflected a liquid crystal display (LCD) screen located at the back of the scanner bore.

3.3. *fMRI object experiment*

In each of the eight runs, participants viewed pictures that were blocked by the five levels of scrambling (S256, S64, S16, S4 and intact) and by category (tools and objects). After an initial fixation of 10.5 sec, the experiment included twenty 9 sec blocks, each comprised of ten stimuli with each image displayed for 600 msec followed by 300 msec fixation. The blocks were separated by 7.5 sec fixation periods. Participants fixated on the cross in the center of the display and performed a task that was orthogonal to the presentation of the objects. Specifically, throughout the scan, participants indicated, via a button press, when the color of the fixation cross changed from black to red. There were one or two fixation color changes randomly occurring per block of ten stimuli.

3.4. *Behavioral object experiment*

Control participants (11 out of 15) and SM (session-1) completed an object recognition experiment after the fMRI scan. The participants sat 50 cm from a computer screen in a darkened room and viewed the same stimuli they had viewed in the scanner. They were instructed to name aloud each stimulus. The experimenter tracked the accuracy of their recognition responses. Stimuli were presented in a pseudo-randomized fashion, for 600 msec (as in the fMRI experiment), with each picture presented once (in contrast to the fMRI experiment, in which objects were blocked).

3.5. *The durability of stored visual representations*

To measure changes in the neural profile of shape sensitivity slopes in SM over time, we rescanned SM 27 months after the first scan using the same paradigm. We also rescanned two of the age-matched controls, with a gap of 38 months between the two scans.

3.6. *Statistical analyses*

3.6.1. *Univariate analysis*

We analyzed the data using BrainVoyager 20.2 software (Brain Innovation, Maastricht, Netherlands), inhouse scripts written in MATLAB (The MathWorks, Inc, Natick, MA, USA) and RStudio (RStudio Team, 2015). Preprocessing included 3D-

motion correction and filtering of low temporal frequencies (cutoff frequency of 2 cycles per run). We did not apply spatial smoothing so as to permit the voxel-wise analysis. We transformed all scans into Montreal Neurological Institute (MNI) space.

The first step of the analytic approach was based on the voxel-wise analysis employed in the previous study (Freud, Culham, et al., 2017). We generated a group-level mask of all visually selective voxels by performing a random-effects general linear model (GLM) analysis across all 15 controls. For each voxel, we tested whether it was reliably responsive to any of the five conditions relative to fixation (scrambling level −S256, S64, S16, S4, Intact; $p < .05$ − FDR corrected). We included all visually sensitive voxels in the mask, which was then applied in the individual subject analysis.

Next, to describe shape sensitivity slopes at the level of each individual voxel, we calculated the linear slope of the activation (beta values) as a function of scrambling level (intact − S256, 5 levels) separately for each participant in each visually selective voxel. A positive slope in a voxel reflects an increase in activation as the level of scrambling decreases (from S256 to intact), and therefore reflects greater shape sensitivity. A negative slope represents a decrease in activation as the level of scrambling decreases, and, as such, may reflect greater sensitivity to local elements and edges, which are more frequent in increasingly distorted images.

3.6.2. *Comparison between SM and controls*

To minimize the number of possible comparisons between SM and controls, we divided the 5624 functional visual voxels that were included in the voxel-wise analysis into 100 clusters based on the physical distance between the voxels. To generate these 100 clusters, we applied 200 iterations of the k-means algorithm on the MNI coordinates of all the functional voxels and selected the results that minimized the sums of point-to-centroid distances. We calculated the slope of each cluster by averaging the voxel-wise slopes across all the voxels included in a particular cluster. Given that our choice of 100 clusters is arbitrary, we repeated this process using 80 clusters and 120 clusters to demonstrate the stability of the reported results.

We adopted two different analytical approaches to evaluate the changes in shape sensitivity in SM compared with the controls. The first approach was designed to generate a spatial description of the regions that were differentially sensitive to shape information in SM compared with the controls. For each cluster, we used the Crawford *t*-test for single cases (Crawford & Howell, 1998) to compare the shape sensitivity slope between SM and controls, and we then averaged the *t* values obtained for SM across the two scans. Finally, to account for the multiple comparisons across the clusters, we also compared each of the controls to all other controls (leave-one-out) to determine whether the number of deviating clusters is greater/lesser in SM compared with the controls creating an ad-hoc false discovery rate.

The second approach explored whether the large-scale organization of shape processing of SM was different from that of controls and we used an inter-subject correlation (ISC) approach (Rosenthal et al., 2017; Simony et al., 2016). ISC is designed to uncover stimulus-locked functional responses, by correlating the response profiles across participants. First, we vectorized the shape sensitivity slopes obtained for all the clusters for each participant (e.g., 100 clusters). Second, we correlated the vector obtained from one participant (e.g., subject 1) with the vector obtained from averaging all remaining participants (e.g., subject 2–15) and repeated this procedure for all participants. Third, we correlated SM's cluster-wise shape sensitivity slope values with each of the leave-one-out mean cluster-wise shape sensitivity slope. We then transformed (Fisher Z) the correlation coefficients and compared the similarity across SM's two scans to the inter-subject similarity observed in controls using the modified Crawford *t*-test for single cases (Crawford & Howell, 1998).

3.6.3. *Longitudinal changes in shape sensitivity slope*

As described above, a shape sensitivity slope was calculated for all visually responsive voxels. Hence, the same voxels (in MNI space) were sampled across scans for those participants who were scanned twice. This approach permitted us to quantify the reliability of the shape sensitivity index by calculating the correlation between the shape sensitivity values across the two scans.

We also evaluated SM's shape sensitivity slopes across the two scans to examine whether there was any change in his shape processing mechanisms over time. To this end, we used the Revised Standardized Difference Test (RSDT) (Crawford & Garthwaite, 2005) that examines the difference between a single-case's scores on two tasks by comparing the difference against the differences observed in a control sample. Note that for most of the control subjects we did not have two scanning sessions, a prerequisite for the RSDT. Hence, we split the control data into odd and even runs and separately calculated shape sensitivity slopes for all clusters.

3.6.4. *Object-recognition task*

We used the Crawford *t*-test for single cases (Crawford & Howell, 1998) to compare behavioral performance in SM compared with control participants.

4. Results

The primary goal of this study was to examine whether a unilateral lesion to the ventral visual pathway alters shape processing computations in the dorsal pathway. We used fMRI to compare shape sensitivity slopes in SM, a patient with visual agnosia following a unilateral lesion to the right ventral pathway, with that of controls. We also explored changes in his neural profile longitudinally to shed light on any potential decrements or improvements.

4.1. *Altered shape sensitivity slopes across both hemispheres and both pathways*

The first analysis was focused on generating a fine-grained mapping of shape sensitivity slopes along the two visual pathways, in SM and in controls. As described previously (Freud, Culham, et al., 2017), for the control individuals, we found robust shape sensitivity slopes in regions along the ventral visual pathway (i.e., lateral occipital cortex, fusiform

gyrus) and along the dorsal visual pathway (i.e., posterior parietal cortex) (Fig. 3A). The sensitivity to shape information in both pathways was observed regardless of the number of clusters that were used (80, 100 or 120 clusters; Figure is shown for 100 clusters, statistical results are presented across the different parcellations) and reflects the distributed nature of shape processing (Freud, Culham, et al., 2017; Freud et al., 2016).

Next, we compared the shape sensitivity slopes in patient SM with that of the control group. We found significant changes in shape sensitivity slopes in both hemispheres and along both visual pathways despite the unilateral nature of his lesion (Fig. 3B). As expected, in comparisons to controls, several regions along the right, lesioned, ventral pathway of SM were less sensitive to shape information (lower slope of beta weights). Significant reduction in shape sensitivity slopes was found in clusters along the Fusiform gyrus and the Parahippocampal gyrus (Fig. 3C upper panel in blue and Table 1 for minimum effect sizes).

Consistent with a previous report (Konen et al., 2011), we also observed reduced shape sensitivity slopes in the left, structurally intact, ventral pathway of SM. In particular, we found significant reduction in shape sensitivity slopes in the lateral aspect of the occipital cortex as well as along the

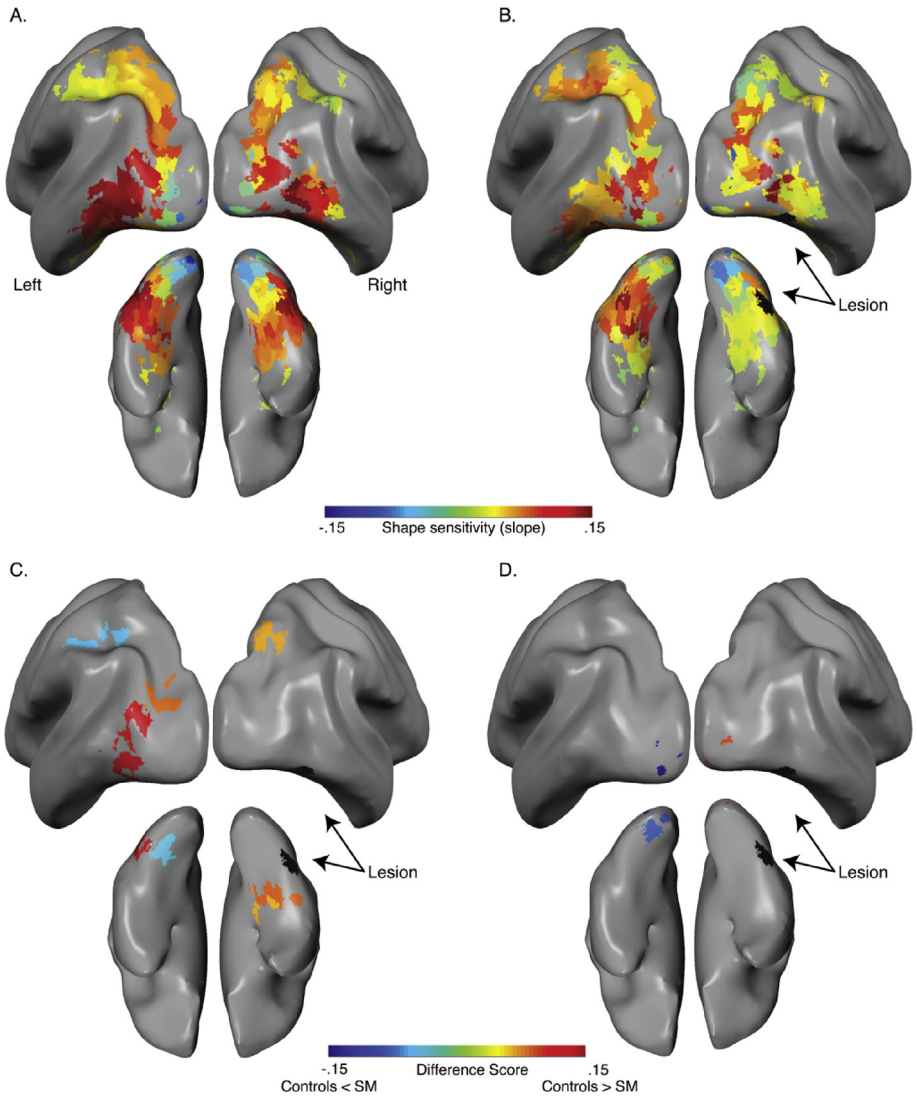

Fig. 3 – Shape sensitivity slopes in the control group and in SM. Shape sensitivity slopes for the control group (A) and SM (averaged across the two scans that were not significantly different from each other, see below) (B) is projected on an inflated brain from a lateral view and from an inferior view, for the right and left hemispheres. Warm colors signify voxels that are shape sensitive, with activation increasing as a function of slope or object coherence. Conversely, cold colors reflect low shape sensitivity (negative slopes) or greater sensitivity for scrambled than intact images. (C–D) Relative to controls, alterations in shape sensitivity slopes in SM were found mainly in shape-selective clusters (slope>0) (C) but also in non-selective clusters (D). Changes were observed across both hemispheres and pathways. SM exhibited reduced shape sensitivity slopes compared with controls (warm colors) in the fusiform gyrus, lateral occipital cortex and superior parietal cortex (bilaterally). Greater shape sensitivity slopes in SM (cold colors) was identified in the left hemisphere in the posterior part of the occipital cortex (i.e., early visual cortex) and in the anterior parietal cortex.

fusiform gyrus (Fig. 3C and D, lower panel in blue and Table 1 for minimum effect sizes).

Importantly, as evident in Fig. 3, the reduction in shape sensitivity slopes in patient SM was not restricted to the ventral pathway. We identified clusters of reduced shape sensitivity slopes in the posterior parts of the Superior Parietal Lobule (SPL) in both hemispheres (Fig. 3C and D, and Table 1 for minimum effect sizes). These results were replicated when the analysis was conducted on different numbers (i.e., 80, 100, 120) of clusters.

It is important to note that the reduced shape sensitivity observed in SM was almost exclusively found in shape-selective clusters that typically exhibit positive slopes [80 clusters − 7 out of 7 clusters; 100 clusters 7 out of 8 clusters; 120 clusters 9 out of 10 clusters]. This finding reinforces the notion that the observed neural processing alterations in SM truly reflects changes in shape processing.

Next, to validate these results, we examined how many clusters with reduced shape sensitivity slopes were observed in each of the controls when compared with all other controls, as a means of creating an ad-hoc false discovery rate and establishing the normal bounds of cluster reduction. For healthy controls, we found an average of 1.73 ± 2.96 (of the 80 cluster analysis), 1.7 ± 2.3 (of the 100 cluster analysis) and 1.6 ± 2.19 (of the 120 cluster analysis) clusters whereas for SM, we identified 7 (of the 80 cluster analysis), 8 (of the 100 cluster) and 10 (of the 120 cluster) significant clusters.

In addition to the clusters that exhibited lower shape sensitivity slopes in SM, somewhat surprisingly, we identified some clusters that were *more* sensitive to shape information in SM (Fig. 3C and D and Table 1). These clusters were found only in the left hemisphere and included early-visual cortex and the anterior portion of the IPS which is usually associated with the planning and execution of grasping movements (Culham et al., 2003; Freud, Macdonald, et al., 2018; Gallivan & Culham, 2015).

Next, we repeated the control analysis and measured how many positively deviating clusters are observed in healthy controls (80 cluster 2.26 ± 2.71; 100 cluster 2.66 ± 3.63; 120 cluster 4 ± 5.11). We note that the number of significant positively deviating clusters in SM was within one standard deviation of that of the controls (80 cluster: SM − 4; 100 cluster: 6; and 120 cluster 5). In light of this, we propose that the greater shape sensitivity slopes in SM should be treated cautiously until further validated.

4.2. *Altered inter-subject correlation in SM*

The first analysis examined whether shape sensitivity slopes were different in SM compared with controls across different regions of the visual cortex. Next, we sought to examine whether the large-scale organization of shape processing in SM differed from that observed in healthy controls. This was accomplished using an Inter-Subject Correlation (ISC) approach (see method for details).

For the controls, we identified a high degree of between-subject similarity and this was true regardless of the number of clusters used (80, 100 or 120 clusters). In contrast, and consistent with the first, cluster-based, analysis, the similarity between SM's shape sensitivity slopes and the average control shape sensitivity slopes was markedly reduced from that observed in controls, again independent of the number of clusters employed [80 clusters (40 per hemisphere):$t_{(14)}$ = -3.16, $p < .01$, $Z\text{-}_{CC} = -3.263$; 100 clusters (50 per hemisphere): $t_{(14)}$ = -3.17, $p < .01$, $Z\text{-}_{CC} = -3.28$; 120 clusters (60 per hemisphere): $t_{(14)}$ = -2.937, $p < .05$, $Z\text{-}_{CC} = -3.034$].

The cluster-based analysis (see above) identified changes in shape processing in both the right and left hemispheres. Furthermore, changes included clusters that were more sensitive to shape information in SM only in the left hemisphere and were not sensitive to such information in controls i.e., clusters in the proximity of the early visual cortex and the anterior Intraparietal Sulcus (aIPS), therefore violating the typical large-scale organization of shape processing in this hemisphere. Hence, we predicted that the ISC analysis would demonstrate that the dissimilarity between SM and controls was mainly mediated by the shape sensitivity slopes profile of the non-lesioned left hemisphere. To examine this prediction, we conducted the ISC analysis separately on each hemisphere and pathway.

We found that the spatial organization of shape sensitivity slopes along the right (lesioned) ventral pathway was similar between SM and controls [80 clusters: $t_{(14)}<1$; 100 clusters: $t_{(14)}<1$; 120 clusters: $t_{(14)} < 1$]. This was also true for the right dorsal pathway [80 clusters: $t_{(14)}<1$; 100 clusters: $t_{(14)}<1$; 120 clusters: $t_{(14)} < 1$]. In contrast, the spatial organization of shape sensitivity slopes along the left, non-lesioned, hemisphere, both in ventral [80 clusters:$t_{(14)}$ = -2.83, $p < .05$, $Z\text{-}_{CC} = -2.926$; 100 clusters: $t_{(14)}$ = -3.486, $p < .01$, $Z\text{-}_{CC} = -3.6$; 120 clusters: $t_{(14)}$ = -2.989, $p < .01$, $Z\text{-}_{CC} = -3.087$] and dorsal pathways [80 clusters:$t_{(14)}$ = -4.469, $p < .01$, $Z\text{-}_{CC} = -4.615$; 100 clusters:

Table 1 − Minimum effect sizes per number of clusters.

	Positive clusters (SM > controls)				Negative clusters (SM < controls)			
	Estimated percentage of the control population obtaining a higher score than SM		Estimated effect size (Z_{CC})		Estimated percentage of the control population obtaining a lower score than SM		Estimated effect size (Z_{CC})	
Number of clusters	% Point	(95% CI)	% Point	(95% CI)	% Point	(95% CI)	% Point	(95% CI)
80	97.7	90.2 to 99.9	2.28	1.29 to 3.25	2.39	.07 to 10.3	−2.23	−3.19 to −1.26
100	97.4	89.3 to 99.9	2.21	1.24 to 3.15	2.4	.07 to 10.5	−2.22	−3.16 to −1.25
120	97.7	90.1 to 99.9	2.27	1.29 to 3.24	2.4	.07 to 10.4	−2.23	−3.18 to −1.25

$t_{(14)} = -5.955$, $p < .01$, $Z\text{-}_{CC} = -5.955$; 120 clusters: $t_{(14)} = -5.245$, $p < .05$, $Z\text{-}_{CC} = -5.417$; Fig. 4A] was markedly different in SM compared with controls. Finally, a RSDT test validated the existence of a dissociation between the left and right hemisphere in patient SM for both the ventral and the dorsal pathway [ventral pathway – $t_{(14)} = 4.85$, $p < .001$; dorsal pathway – $t_{(14)} = 9.93$, $p < .001$].

An in-depth examination of the changes in shape sensitivity slopes as a function of the location of the ROIs on the posterior–anterior axis of the brain (as done before, see Freud, Culham, et al., 2017) provides important insights for the results described above. In particular, for controls, both pathways, across both hemispheres followed a two-linear-components function such that shape sensitivity slopes

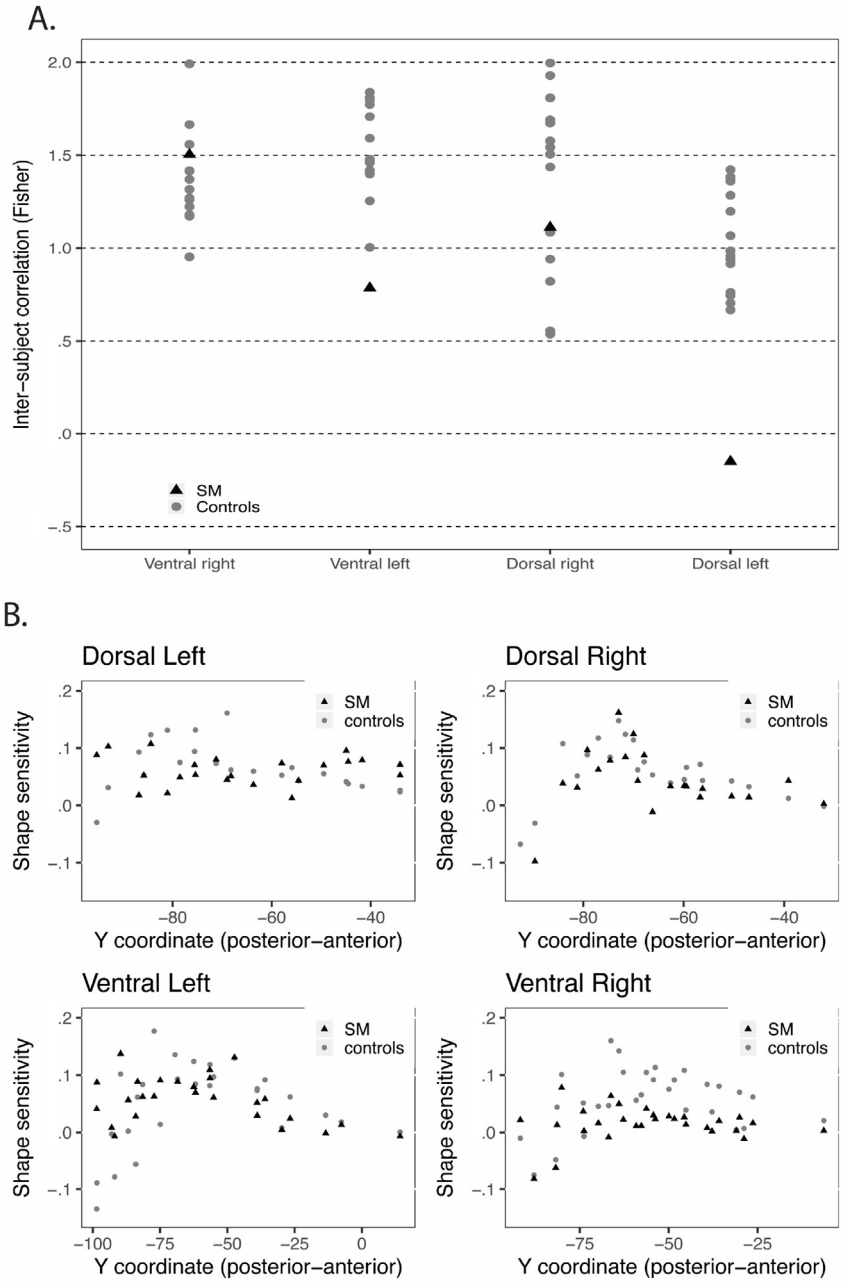

Fig. 4 – Inter-Subject Correlation (ISC) results- A. ISC analysis revealed high similarity of shape sensitivity slopes between control participants and, for SM, reduced similarity was found in the left ventral and dorsal pathway. Each gray circle represents one control participant, while the black triangles represent SM's similarity indices. B. Shape sensitivity slopes of all ROIs in each pathway is plotted against the Y coordinate (posterior–anterior axis) for controls' group average (gray circles) and SM (black triangles). In the left hemisphere, across both pathways, SM exhibited different spatial organization of shape sensitivity slopes than controls. On the other hand, along the right hemisphere, reduction in shape sensitivity was observed in SM, but the general spatial organization of shape sensitivity slopes was preserved.

increased from early visual cortex to extrastriate cortex but then decreased in anterior regions. In SM, this spatial distribution of shape sensitivity slopes was preserved mediating the similarity observed in the ISC analysis, notwithstanding the reduction of shape sensitivity slopes in shape-selective ROIs. In contrast, in the left hemisphere (across both pathways), SM spatial organization was remarkably different with posterior ROIs (across both pathways) and anterior ROIs (along the dorsal pathway) demonstrating an enhanced sensitivity to shape information relative to controls (Fig. 4B).

Collectively, these results provide novel evidence that a lesion to the ventral right pathway can alter shape processing in distal cortical locations, such as in the homologous left ventral hemisphere and in the left dorsal pathway.

4.3. *Longitudinal changes in SM shape sensitivity slopes*

The robustness of the parametric scrambling manipulation allowed us (Freud, Culham, et al., 2017; Freud et al., 2019) and others (Lerner et al., 2001) to map the neural correlates of shape processing in healthy adults and children. Here, we adopted this paradigm both to characterize the neural basis of shape sensitivity in a patient with visual agnosia, and to examine possible longitudinal changes (and test-retest reliability) to the functional neural profile in this patient. Both SM and two control participants were scanned twice, and we computed correlations across the two scans.

First, for each individual, we correlated the two scans to establish the reliability of shape sensitivity slopes indices across the scans. SM, as well as the two matched controls, showed substantial reliability between the two scans and the correlations between shape sensitivity slopes indices over the two scans were high [rs > .78, $ts_{(5623)} > 93$, $p < .0001$; see below for values for each individual] reflecting the reliability and robustness of the scrambling procedure (Fig. 5).

Next, we examined whether SM's shape sensitivity slopes differed in scan 1 and scan 2. Overall, there were no apparent significant changes in shape sensitivity. This was true across all clusters, and independent of the number of clusters that were utilized (80 clusters, max $t_{(14)} = 1.66$, $p = .11$; 100 clusters $t_{(14)} = 1.2$, $p = .24$; 120 clusters $t_{(14)} = 1.6$, $p = .13$). These results attest to the stability of shape sensitivity in SM over two years.

4.4. *Behavioral performance*

The behavioral results of the controls were reported in a previous paper (Freud, Culham, et al., 2017). In short, we found that object recognition accuracy decreased as scrambling increased, as revealed by a main effect of scrambling level in the repeated measures ANOVA [$F_{(1,10)} = 477$, $p = .000001$, $\eta_p^2 = .97$]. Controls accurately identified 97% of the intact images, and their performance decreased as less shape information was available (e.g., 85% for S4 and only 28% for S64).

SM was tested once, after his first fMRI scan. Unsurprisingly, his performance was poor compared to the controls (Fig. 6). He recognized only 61% of the intact objects [single-case comparison - $t_{(14)} = -11.942$, $p < .0001$, effect size: Z-cc = −12.33], and his performance dropped precipitously to 9% for the 4S condition [$t_{(14)} = -10.789$, $p < .0001$, effect size: Z-cc = −11.14]. SM's values were lower than those of the controls for all other levels, as well (excluding the most scrambled S256 condition in which controls average accuracy was 5%). Together, SM's behavioral results are consistent with the fMRI data and reflect SM's poor sensitivity to shape information.

5. Discussion

The processing of shape information is supported by a network of regions extending from the early visual cortex to both the ventral and dorsal visual pathway. Notwithstanding this wide distribution, a lesion to the ventral pathway alone, can lead to visual agnosia, questioning the contribution of the dorsal pathway to object perception. In the current study, we addressed this issue by investigating how a lesion to one pathway (and one hemisphere) impacts shape processing in different parts of the cortical visual system. Additionally, we examined whether shape processing mechanisms were subject to longitudinal changes in a case of visual agnosia.

5.1. *Distributed and interactive shape representations*

We employed a parametric box-scrambling manipulation to characterize shape processing mechanisms in SM, a patient suffering from persistent visual agnosia, after a unilateral lesion sustained to the right ventral visual pathway. We utilized two complementary analytical approaches to generate a

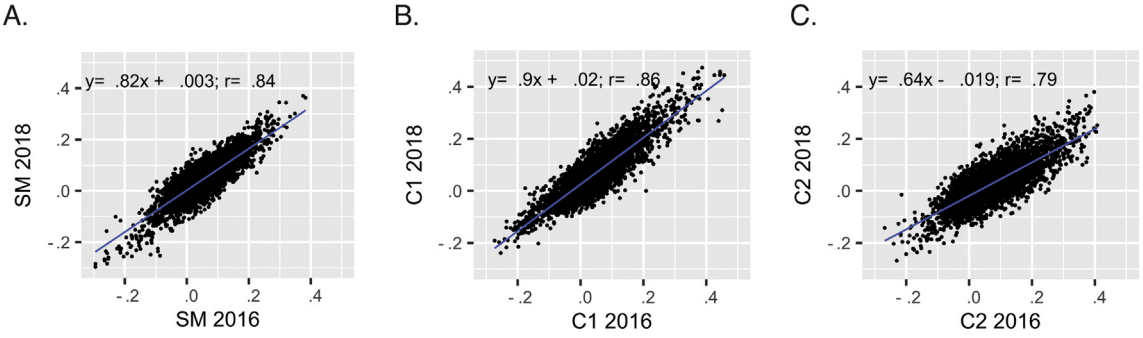

Fig. 5 – Longitudinal stability in shape sensitivity slopes in SM (A) and two matched controls (B–C). Voxel-wise shape sensitivity slopes indices were correlated across the two scans. In all three participants, high correlations were found between scans. SM's shape sensitivity slopes remained stable across the two scans.

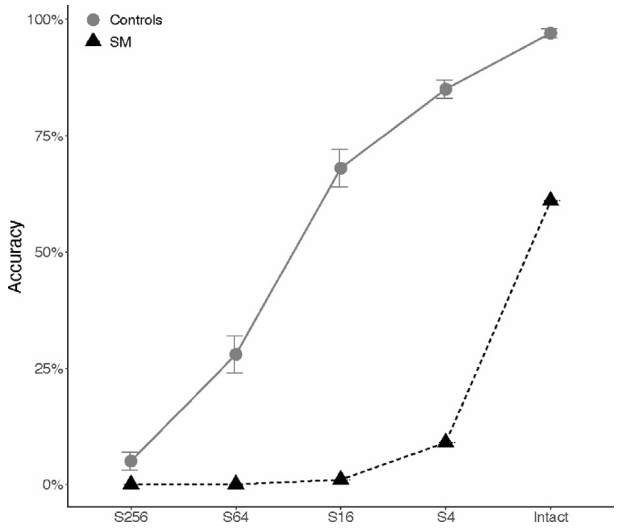

Fig. 6 – Object recognition performance. Mean accuracy of recognition as a function of scrambling using data obtained outside the scanner. Recognition accuracy decreased as a function of scrambling in controls and in SM. SM performed poorly, relative to controls, across all levels of scrambling excluding the most scrambled version (due to a floor effect).

fine-grained map of shape sensitivity slopes in SM and to compare the large-scale organization of shape processing along the two visual pathways.

The results of these analyses reveal reduced shape sensitivity slopes in the anterior parts of the ventral pathway in the right (lesioned) as well as the left (non-lesioned) hemispheres. Additionally, we observed bilateral reduced shape sensitivity slopes in the superior parts of the dorsal pathway. Finally, some indications for enhanced shape sensitivity slopes in SM compared with controls, were observed along the left hemisphere. These results were corroborated by the inter-subject correlation analysis that revealed changes in the large-scale spatial organization of shape processing in SM left hemisphere.

Collectively, these results provide novel evidence for the neural basis of shape processing. In particular, we show that a unilateral lesion to the ventral pathway can adversely impact shape processing mechanisms in both hemispheres and in both visual pathways. This pattern of results provides support for the third hypothesis outlined in the introduction, according to which, shape perception may rely on representations derived by the ventral and dorsal pathways (Erlikhman, Caplovitz, Gurariy, Medina, & Snow, 2018; Freud et al., 2016). These representations are likely to be different from each other (Bracci & Op de Beeck, 2016; Freud et al., 2020), but their interactive or interdependent nature makes them susceptible to alterations when a lesion is sustained to one of the pathways.

This conclusion is consistent with recent evidence from an electrophysiology study in nonhuman primates that showed that reversible inactivation of the caudal intraparietal sulcus led to decreased fMRI activation in the anterior parts of the ventral pathway in response to 3D stimuli (Van Dromme et al., 2016). Also, a recent neuropsychological investigation, conducted with a patient who had sustained a lesion to the anterior parietal cortex, uncovered a reduction or impairment in tool processing in the ventral pathway (Garcea et al., 2019). Notably, these studies have demonstrated the reverse alteration of visual processing to that reported here, as the function of the ventral pathway was altered by a lesion of the dorsal pathway. Together with the results of the current study, we suggest that visual processing relies on bidirectional connections between the two visual pathways and two hemispheres.

The current results are inconsistent with a previous study in which we demonstrated that, in patients with visual agnosia following a lesion to the ventral pathway, the dorsal pathway continues to evince sensitivity to object 3D structure and this is true even in a case with a very extensive bilateral ventral lesion (Freud, Ganel, et al., 2017). This apparent inconsistency might be explained, however, by the focus of the previous paper on one, high-level, shape property (i.e., 3D structure), while the current paper is focused on more fundamental shape computations. In other words, dorsal cortex may derive 3D information independently on ventral cortex, but other properties of shape may require an integration between ventral and dorsal cortices. An additional plausible explanation relates to the different analytical pipeline adopted in these studies. While the previous study focused on particular, pre-defined, object-selective ROIs along the dorsal pathway, the current paper explores shape processing along the whole dorsal pathway providing superior spatial coverage. This might suggest that certain dorsal regions do derive information independently of ventral cortex (e.g., regions IPS 1–2 that were found to have differential representational structures from ventral pathway regions; Freud, Culham, et al., 2017) but other dorsal regions interact or are even coupled with ventral regions (e.g., IPS-0). Future research should explore whether the inter-pathway interactions are modulated by the nature of the task, visual stimulation and whether there are specific regions that play a key role in the interactions between the two pathways.

5.2. *The role of diaschisis in visual agnosia*

The term diaschisis, coined by von Monakow in 1914 refers to neural and neuropsychological changes expressed in a distal region following a focal brain lesion. Over the years, evidence for diaschisis following a sub-cortical lesion (Lim, Ryu, Kim, & Lee, 1998) has been demonstrated, and, with the advent of non-invasive metabolic imaging techniques (such as fMRI), evidence for corticocortical diaschisis has been reported (Carrera & Tononi, 2014; Price, Warburton, Moore, Frackowiak, & Friston, 2001).

The fMRI activation profile observed for patient SM clearly reflects functional diaschisis, with alterations in the neural profile in remote cortical regions in response to visual stimulation. To the best of our knowledge, the current results, which extend the previous report on patient SM (Konen et al., 2011), are the first to reveal functional diaschisis in visual agnosia. This interpretation can also explain why visual agnosia is observed even in cases of unilateral lesion. That is,

even a circumscribed, unilateral, lesion to one region (in the case of SM, the inferior portion of the LOC) can lead to widespread, bilateral, changes in shape processing.

That visual processing can be subject to functional diaschisis is consistent with a recent report that showed alteration of neural processing of tool images by the ventral pathway after lesions to the dorsal pathway (Garcea et al., 2019). Given this accumulating evidence, future research should investigate whether functional diaschisis is also observed in other cases of acquired visual impairments such as prosopagnosia and pure alexia which also occur following a ventral lesion.

An outstanding question regards to the neural mechanisms that give rise to the observed pattern of wide alterations across the two pathways and the two hemispheres. One option is that the structural and functional connectivity patterns of the lesioned region determine the long-term changes in shape processing of distal regions. Previous studies have already demonstrated the existence of structural and functional connections between the two pathways (Freud et al., 2015; Hutchison & Gallivan, 2018; Yeatman et al., 2014) in addition to robust homotopic connections between the hemispheres (Biswal, Yetkin, Haughton, & Hyde, 1995).

Consistently, connectivity patterns are assumed to shape the development of visual representations along the ventral visual pathway (Behrmann & Plaut, 2013). Moreover, it was found that alterations of the typical connectivity play a central role in other perceptual deficits such as congenital prosopagnosia, where reduced structural connections between the FFA and the anterior temporal cortex (Thomas et al., 2009) are accompanied by large-scale changes in the connectivity patterns of the face-selective network (Rosenthal et al., 2017). Thus, it is plausible, that the distal effects of the right LOC lesion observed here, are based on the connections to and from this region.

5.3. *Stability of shape sensitivity slopes over-time*

The study of longitudinal changes in agnosia is interesting for several reasons. Our findings from two fMRI scans conducted two years apart revealed a high degree of similarity in shape sensitivity slopes in both dorsal and ventral cortex. This result attests to the test-retest reliability of our approach and is likely to be expected given that the two scans were both performed roughly two decades after the brain damage.

To date, there have been rather few systematic longitudinal studies of agnosia and none has collected neuroimaging data. In all cases, behavioral testing showed that the improvement was limited. Of note too is that the temporal interval over which the improvement is observed varies dramatically. In the case of HC, the minimal improvement happened within the first 6 months post-anoxic damage whereas for JR, there was steady, albeit limited, improvement over 10 years. Over 16 years, HJA, and, over 10 years, Kertesz's patient (1979) showed minor improvement especially evident in real object recognition, likely a compensatory use of 3D, color and texture information (Riddoch et al., 1999, 2003). Even in those cases with some improvement, this has been generally attributed to the use of compensatory cues and there is still evidence of limitations in long-term knowledge as in patient JR (Davidoff & Wilson, 1985; Wilson & Davidoff, 1993) and patient HC (Adler, 1944, 1950; Sparr et al., 1991).

In one final longitudinal study, in an effort to determine more specifically what changes are potentially possible in agnosia over time, DW was initially tested 3 years after he sustained a head injury (during an epilepsy incident) and then tested 12 years later (Thomas, Forde, Humphreys, & Graham, 2002). Like HJA and Kertesz's patient, DW did improve in his ability to identify real objects compared to line drawings but his category-specific agnosia for living things remained unchanged. Interestingly, as in the case of HJA, DW's access to stored knowledge of shape appeared to decline. Together, these agnosia cases provide a compelling argument for the claim that in the absence of perceptual input, stored visual knowledge cannot be updated and, at best, will remain unchanged or may even degenerate over time.

Because we do not have very detailed behavioral assessment for SM over time and given the extended period of time from the injury, we are limited in deciding whether his behavioral profile is one of improvement or deterioration (or stability). We have shown, however, that, unlike these other studies of agnosia which do not have neuroimaging data, SM's BOLD profile remains unchanged. Clearly, much more work is required both empirically so that behavior and neural data are collected in tandem, and theoretically in order to determine whether perceptual bottom-up input is necessary to maintain stored representations.

5.4. *Limitations*

Despite the novel findings of the current research, several important limitations should be taken into account. First, the cluster-based analysis revealed several clusters that were more sensitive to shape information in SM compared with controls (i.e., positively deviating clusters). However, such deviating clusters were also observed in some of the controls, raising the concern that the positively deviating clusters in SM reflect false alarms or simply fall within the variability range of normal controls. It is noteworthy though that the positively deviating clusters in SM were found in both scans and appeared in the left, non-lesioned, hemisphere, and not in regions that are homologous to the lesion location, reinforcing the notion that these clusters might support compensatory mechanisms that support residual perceptual abilities.

Another potential limitation concerns the longitudinal investigation of shape processing profile in SM. While we were unable to identify any changes in the neural profile of shape processing across the two scans (despite the high reliability of the dependent variable) conducted two years apart. It is important to note that SM's injury was sustained roughly 20 years ago, and, therefore, it is possible that any longitudinal changes in shape processing had already occurred at an earlier time point and reached asymptote. Therefore, to gain greater traction on this issue, future research should map longitudinal changes in visual processing in cases of brain injuries earlier in the course of the neuropsychological trajectory.

6. Conclusions

The neural mechanisms that support shape processing include regions along the dorsal and ventral visual pathways.

Here, we show that a circumscribed lesion to the right ventral pathway can have large-scale adverse effects on shape processing along both the ventral and dorsal pathways and in both the affected and preserved hemispheres. These changes remained stable across a two-year interval. Together, these findings are consistent with the claim that a distributed network of regions, along both visual cortical pathways, contributes to shape perception.

CRediT author statement

Erez Freud- Conceptualization, Methodology, Formal analysis, Writing - Original Draft, Writing - Review & Editing, Visualization, Funding acquisition

Marlene Behrmann- Conceptualization, Methodology, Writing - Review & Editing, Supervision, Funding acquisition

Open practices

The study in this article earned Open Materials and Open Data badges for transparent practices. Materials and data for the study are available at https://figshare.com/collections/The_large-scale_organization_of_shape_processing_in_the_ventral_and_dorsal_pathways/3889873.

Declaration of Competing Interest

The authors declare no competing interests.

Acknowledgements

This research was funded by NIH R01EY026701 (MB), by Natural Sciences and Engineering Research Council of Canada (NSERC) (EF) and by the Vision Science to Applications (VISTA) program funded by the Canada First Research Excellence Fund (CFREF, 2016–2023) (EF).

We thank SM for his continued participation.

REFERENCES

Adler, A. (1944). Disintegration and restoration of optic recognition in visual agnosia: Analysis of a case. *Archives of Neurology & Psychiatry, 51*(3), 243–259.

Adler, A. (1). Course and outcome of visual agnosia. *The Journal of Nervous and Mental Disease, 111*, 41–51. https://doi.org/10.1097/00005053-195011110-00004.

Andrew, A. M. (1979). Another efficient algorithm for convex hulls in two dimensions. *Information Processing Letters, 9*(5), 216–219. https://doi.org/10.1016/0020-0190(79)90072-3.

Behrmann, M., & Kimchi, R. (2003). What does visual agnosia tell us about perceptual organization and its relationship to object perception? *Journal of Experimental Psychology: Human Perception and Performance, 29*(1), 19–42.

Behrmann, M., & Plaut, D. C. (2013). Distributed circuits, not circumscribed centers, mediate visual recognition. *Trends in Cognitive Sciences, 17*(5), 210–219.

Behrmann, M., & Plaut, D. C. (2014). Bilateral hemispheric processing of words and faces: Evidence from word impairments in prosopagnosia and face impairments in pure alexia. *Cerebral Cortex, 24*(4), 1102–1118. https://doi.org/10.1093/cercor/bhs390.

Biswal, B., Yetkin, F. Z., Haughton, V. M., & Hyde, J. S. (1995). Functional connectivity in the motor cortex of resting human brain using echo-planar MRI. *Magnetic Resonance in Medicine, 34*, 537–541.

Bracci, S., & Op de Beeck, H. (2016). Dissociations and associations between shape and category representations in the two visual pathways. *The Journal of Neuroscience, 36*(2), 432–444. https://doi.org/10.1523/JNEUROSCI.2314-15.2016.

Carrera, E., & Tononi, G. (2014). Diaschisis: Past, present, future. *Brain, 137*(9), 2408–2422.

Collins, E., Freud, E., Kainerstorfer, J. M., Cao, J., & Behrmann, M. (2019). Temporal dynamics of shape processing differentiate contributions of dorsal and ventral visual pathways. *Journal of Cognitive Neuroscience, 31*(6), 821–836.

Crawford, J. R., & Garthwaite, P. H. (2005). Testing for suspected impairments and dissociations in single-case studies in neuropsychology: Evaluation of alternatives using Monte Carlo simulations and revised tests for dissociations. *Neuropsychology, 19*(3), 318–331.

Crawford, J. R., & Howell, D. C. (1998). Comparing an individual's test score against norms derived from small samples. *The Clinical Neuropsychologist, 12*(4), 482–486.

Culham, J. C., Danckert, S. L., De Souza, J. F., Gati, J. S., Menon, R. S., & Goodale, M. A. (2003). Visually guided grasping produces fMRI activation in dorsal but not ventral stream brain areas. *Experimental Brain Research, 153*(2), 180–189. https://doi.org/10.1007/s00221-003-1591-5.

Davidoff, J., & Wilson, B. (1985). A case of visual agnosia showing a disorder of pre-semantic visual classification. *Cortex, 21*(1), 121–134.

Erlikhman, G., Caplovitz, G. P., Gurariy, G., Medina, J., & Snow, J. C. (2018). Towards a unified perspective of object shape and motion processing in human dorsal cortex. *Consciousness and Cognition, 64*, 106–120.

Freud, E., Behrmann, M., & Snow, J. C. (2020). What does dorsal cortex contribute to perception? *Open Mind* (In press).

Freud, E., Culham, J. C., Plaut, D. C., & Behrmann, M. (2017a). The large-scale organization of shape processing in the ventral and dorsal pathways. *ELife, 6*, e27576. https://doi.org/10.7554/eLife.27576.

Freud, E., Ganel, T., Shelef, I., Hammer, M. D., Avidan, G., & Behrmann, M. (2017b). Three-dimensional representations of objects in dorsal cortex are dissociable from those in ventral cortex. *Cerebral Cortex, 27*(1), 422–434. https://doi.org/10.1093/cercor/bhv229.

Freud, E., Macdonald, S. N., Chen, J., Quinlan, D. J., Goodale, M. A., & Culham, J. C. (2018a). Getting a grip on reality: Grasping movements directed to real objects and images rely on dissociable neural representations. *Cortex, 98*, 34–48. https://doi.org/10.1016/j.cortex.2017.02.020.

Freud, E., Plaut, D. C., & Behrmann, M. (2016). 'What' is happening in the dorsal visual pathway. *Trends in Cognitive Sciences, 20*(10), 773–784. https://doi.org/10.1016/j.tics.2016.08.003.

Freud, E., Plaut, D. C., & Behrmann, M. (2019). Protracted developmental trajectory of shape processing along the two visual pathways. *Journal of Cognitive Neuroscience, 1–9*.

Freud, E., Robinson, A. K., & Behrmann, M. (2018b). More than action: The dorsal pathway contributes to the perception of 3-D structure. *Journal of Cognitive Neuroscience, 30*(7), 1047–1058.

Freud, E., Rosenthal, G., Ganel, T., & Avidan, G. (2015). Sensitivity to object impossibility in the human visual cortex: Evidence from functional connectivity. *Journal of Cognitive Neuroscience, 27*(5), 1029–1043. https://doi.org/10.1162/jocn_a_00753.

Gallivan, J. P., & Culham, J. C. (2015). Neural coding within human brain areas involved in actions. *Current Opinion in Neurobiology, 33*, 141–149. https://doi.org/10.1016/j.conb.2015.03.012.

Garcea, F. E., Almeida, J., Sims, M. H., Nunno, A., Meyers, S. P., Li, Y. M., et al. (2019). Domain-specific diaschisis: Lesions to parietal action areas modulate neural responses to tools in the ventral stream. *Cerebral Cortex, 29*(7), 3168–3181. https://doi.org/10.1093/cercor/bhy183.

Garcea, F. E., Chen, Q., Vargas, R., Narayan, D. A., & Mahon, B. Z. (2018). Task-and domain-specific modulation of functional connectivity in the ventral and dorsal object-processing pathways. *Brain Structure & Function, 223*(6), 2589–2607.

Gilaie-Dotan, S., Saygin, A. P., Lorenzi, L. J., Egan, R., Rees, G., & Behrmann, M. (2013). The role of human ventral visual cortex in motion perception. *Brain, 136*(9), 2784–2798.

Gilaie-Dotan, S., Saygin, A. P., Lorenzi, L. J., Rees, G., & Behrmann, M. (2015). Ventral aspect of the visual form pathway is not critical for the perception of biological motion. *Proceedings of the National Academy of Sciences, 112*(4), E361–E370. https://doi.org/10.1073/pnas.1414974112.

Goodale, M. A., Milner, A. D., Jakobson, L. S., & Carey, D. P. (1991). A neurological dissociation between perceiving objects and grasping them. *Nature, 349*(6305), 154–156.

Grill-Spector, K., Kushnir, T., Hendler, T., Edelman, S., Itzchak, Y., & Malach, R. (1998). A sequence of object-processing stages revealed by fMRI in the human occipital lobe. *Humum Brain Mapping, 6*, 316–328. https://doi.org/10.1002/(SICI)1097-0193(1998)6:4<316::AID-HBM9>3.0.CO;2-6.

Humphreys, G. W., & Riddoch, M. J. (1984). Routes to object constancy: Implications from neurological impairments of object constancy. *The Quarterly Journal of Experimental Psychology, 36*(3), 385–415.

Humphreys, G. W., & Riddoch, M. J. (1987). The fractionation of visual agnosia. In *Visual object processing: A cognitive neuropsychological approach* (pp. 281–306). Lawrence Erlbaum Associates, Inc.

Hutchison, R. M., & Gallivan, J. P. (2018). Functional coupling between frontoparietal and occipitotemporal pathways during action and perception. *Cortex, 98*, 8–27.

Kertesz, A. (1979). Visual agnosia: The dual deficit of perception and recognition. *Cortex, 15*(3), 403–419.

Konen, C. S., Behrmann, M., Nishimura, M., & Kastner, S. (2011). The functional neuroanatomy of object agnosia: A case study. *Neuron, 71*(1), 49–60. https://doi.org/10.1016/j.neuron.2011.05.030.

Konen, C. S., & Kastner, S. (2008). Two hierarchically organized neural systems for object information in human visual cortex. *Nature Neuroscience, 11*(2), 224–231. https://doi.org/10.1038/nn2036.

Lerner, Y., Hendler, T., Ben-Bashat, D., Harel, M., & Malach, R. (2001). A hierarchical axis of object processing stages in the human visual cortex. *Cerebral Cortex, 11*, 287–297. https://doi.org/10.1093/cercor/11.4.287.

Lim, J. S., Ryu, Y. H., Kim, B. M., & Lee, J. D. (1998). Crossed cerebellar diaschisis due to intracranial hematoma in basal ganglia or thalamus. *Journal of Nuclear Medicine, 39*(12), 2044–2047.

Mahon, B. Z., Kumar, N., & Almeida, J. (2013). Spatial frequency tuning reveals interactions between the dorsal and ventral visual systems. *Journal of Cognitive Neuroscience, 25*(6), 862–871. https://doi.org/10.1162/jocn_a_00370.

Malach, R., Reppas, J. B., Benson, R. R., Kwong, K. K., Jiang, H., Kennedy, W. A., et al. (1995). Object-related activity revealed by functional magnetic resonance imaging in human occipital cortex. *Proceedings of the National Academy of Sciences of the United States of America, 92*, 8135–8139.

Marotta, J. J., Genovese, C. R., & Behrmann, M. (2001). A functional MRI study of face recognition in patients with prosopagnosia. *Neuroreport, 12*(8), 1581–1587.

Nishimura, M., Doyle, J., Humphreys, K., & Behrmann, M. (2010). Probing the face-space of individuals with prosopagnosia. *Neuropsychologia, 48*(6), 1828–1841.

Price, C. J., Warburton, E. A., Moore, C. J., Frackowiak, R. S. J., & Friston, K. J. (2001). Dynamic diaschisis: Anatomically remote and context-sensitive human brain lesions. *Journal of Cognitive Neuroscience, 13*(4), 419–429.

Riddoch, M. J., & Humphreys, G. W. (1987). A case of integrative visual agnosia. *Brain, 110*(6), 1431–1462.

Riddoch, M. J., Humphreys, G. W., Blott, W., Hardy, E., Smith, A. D., & Smith, A. D. (2003). Visual and spatial short-term memory in integrative agnosia. *Cognitive Neuropsychology, 20*(7), 641–671.

Riddoch, M. J., Humphreys, G. W., Gannon, T., Blott, W., & Jones, V. (1999). Memories are made of this: The effects of time on stored visual knowledge in a case of visual agnosia. *Brain, 122*(3), 537–559.

Rosenthal, G., Tanzer, M., Simony, E., Hasson, U., Behrmann, M., & Avidan, G. (2017). Altered topology of neural circuits in congenital prosopagnosia. *Elife, 6*, e25069.

RStudio Team. (2015). *RStudio*. Boston, MA: Integrated Development for R. http://www.rstudio.com/.

Simony, E., Honey, C. J., Chen, J., Lositsky, O., Yeshurun, Y., Wiesel, A., et al. (2016). Dynamic reconfiguration of the default mode network during narrative comprehension. *Nature Communications, 7*, 12141. https://doi.org/10.1038/ncomms12141.

Sparr, S. A., Jay, M., Drislane, F. W., & Venna, N. (1991). A historic case of visual agnosia revisited after 40 years. *Brain, 114*(2), 789–800.

Thomas, C., Avidan, G., Humphreys, K., Jung, K., Gao, F., & Behrmann, M. (2009). Reduced structural connectivity in ventral visual cortex in congenital prosopagnosia. *Nature Neuroscience, 12*(1), 29.

Thomas, R. M., Forde, E. M., Humphreys, G. W., & Graham, K. S. (2002). A longitudinal study of category-specific agnosia. *Neurocase, 8*(6), 466–479.

Van Dromme, I. C., Premereur, E., Verhoef, B.-E., Vanduffel, W., & Janssen, P. (2016). Posterior parietal cortex drives inferotemporal activations during three-dimensional object vision. *Plos Biology, 14*(4), e1002445. https://doi.org/10.1371/journal.pbio.1002445.

Vaziri-Pashkam, M., & Xu, Y. (2018). An information-driven 2-pathway characterization of occipitotemporal and posterior parietal visual object representations. *Cerebral Cortex, 29*(5), 2034–2050.

Wilson, B. A., & Davidoff, J. (1993). Partial recovery from visual object agnosia: A 10 year follow-up study. *Cortex, 29*(3), 529–542.

Yeatman, J. D., Weiner, K. S., Pestilli, F., Rokem, A., Mezer, A., & Wandell, B. A. (2014). The vertical occipital fasciculus: A century of controversy resolved by in vivo measurements. *Proceedings of the National Academy of Sciences, 111*(48), E5214–E5223. https://doi.org/10.1073/pnas.1418503111.